Monte Carlo Simulation of a Homopolymer−Copolymer Mixture Interacting with a Surface: Bulk versus Surface Micelles and Brush Formation

A. Cavallo,*,†,‡ M. Müller,§ and K. Binder†

Institut für Physik, Johannes-Gutenberg-Universität, Staudingerweg 7, D-55099 Mainz, Germany, Institut Charles Sadron, 23, rue du Loess, F-67034 Strasbourg, France, and Institut für Theoretische Physik, Friedrich-Hund-Platz 1, Georg-August-Universität, D-37077 Göttingen, Germany

Received February 4, 2008; Revised Manuscript Received April 16, 2008

ABSTRACT: Using Monte Carlo simulations of the bond fluctuation model, we study the formation of micelles in a confined mixture of asymmetric AB-diblock copolymers and homopolymers. The composition of the sphere-forming AB-diblock copolymers is $f_A = 1/8$. The mixture is confined into a thin film. The film surfaces attract the minority component of the diblock with strength, ε_W. To efficiently sample the micelle size distribution and establish equilibrium between the surface and the bulk, we work in the semigrandcanonical ensemble, i.e. at fixed density and fixed chemical potential difference between the two types of chains, choosing a large incompatibility $\chi N \simeq 100$ (strong segregation regime). The composition of the mixture is controlled by the chemical potential difference, $\delta\mu = \mu_{cop} - \mu_{hom}$, between copolymers and homopolymers. We study the morphology as a function of the surface interaction, ε_W, and the chemical potential, $\delta\mu$. Only in a limited regime of parameters—i.e., in the vicinity of the adsorption transition of the minority component at the surface and slightly below the critical micelle concentration in the bulk—surface micelles are formed. We characterize the shape of the adsorbed micelles by the tensor of gyration and radial density profiles.

I. Introduction

The adsorption of amphiphilic molecules at surfaces and interfaces has attracted abiding interest because already a small volume fraction of amphiphiles in the bulk can give rise to a large surface excess, which, in turn, significantly alters the interface properties.[1] The adsorption of amphiphiles at surfaces or interfaces is utilized to reduce the interface tension between two coexisting phases,[2,3] alter the bending rigidity,[4,5] tailor the wettability, or tune the hydrodynamic boundary condition and produce slip. The interplay between micelle formation in the bulk and the adsorption of amphiphiles onto surfaces is important because the formation of micelles in the bulk might considerably slow down the transport of amphiphiles toward the surface.[6−10] In order to achieve fast equilibration, it may be advantageous to identify thermodynamic conditions where the surface excess of amphiphiles is large but the concentration of amphiphiles in the bulk is below the critical micelle concentration. These conditions are also of interest for structuring surfaces with micellar aggregates.[6,9,11−19]

The properties of the adsorbed layer of amphiphiles depend on the bulk concentration and the interaction between the amphiphiles and the surface. In the limit of long macromolecules, two distinct transitions can be distinguished: (i) In the limit of small bulk concentration, one encounters an adsorption transition[20] of the block that is attracted to the surface upon increasing the attraction between the surface and the preferred block. Below this threshold, the surface excess of amphiphiles is small, and above it rapidly increases as one increases the strength of the attraction. (ii) As one increases the concentration of amphiphilic molecules in the bulk, micelles form at the critical micelle concentration (cmc);[21,22] i.e., below the cmc, amphiphilic molecules remain isolated in solution while above the cmc they aggregate into micelles. The interplay between these two phenomena dictates the behavior of the amphiphilic molecule at the surface. For finite chain length, the transitions are rounded and replaced by gradual cross-overs between distinct regimes.

The interplay between adsorption and micellization in the bulk has been studied by Monte Carlo simulations.[7] In the following, we focus on the structure at the surface of an amphiphilic solution slightly below the cmc, where there are only few, isolated amphiphilic molecules in the bulk. Then, the adsorbed surface layer may consist of adsorbed, isolated molecules, or clusters of molecules, or a dense layer of amphiphiles. The latter two morphologies will be denoted "surface micelle" and "absorbed brush", respectively.

Previous studies have explored the lateral structure of adsorbed layers of block copolymers by theoretical considerations and simulations,[13,15,16] and the results have been compared with experimental data. In these studies, the areal density of copolymers at the surface has been fixed. The formation of noninteracting surface micelles by adsorption of block copolymers from a selective solvent has been theoretically investigated within a Flory-type approximation[11] and using Monte Carlo simulations.[14] However, due to the difficulties of equilibration only very short chains could be studied in the latter work.

In the present work, the surface is in equilibrium with a bulk solution, i.e., the adsorbed layer and the bulk can exchange amphiphiles. Moreover, the nonadsorbing block is long and forms the corona in the good solvent. We explore under which thermodynamic conditions a surface excess can be obtained that will give rise to a laterally structured, adsorbed layer.

We use Monte Carlo simulations of a coarse-grained lattice model to systematically explore the behavior of the adsorbed amphiphilic layer as a function of the surface interaction and the bulk concentration. The mixture is comprised of a sphere-forming, asymmetric AB-diblock copolymer and a homopolymer−solvent of identical chain length. Using the semigrandcanonical ensemble, we are able to efficiently equilibrate large systems of long chains and establish chemical equilibrium between surface and solution formed by homopolymers of the

* Corresponding author.
† Institut für Physik, Johannes-Gutenberg-Universität.
‡ Institut Charles Sadron.
§ Institut für Theoretische Physik, Georg-August-Universität.

10.1021/ma800262f CCC: $40.75
Published on Web 06/10/2008

same chain length. We characterize the size and shape of the surface micelles and obtain a qualitative phase diagram.

Our manuscript is arranged as follows: In the next section we introduce our model and simulation technique. Then, we investigate the adsorption of the amphiphiles from the bulk and present evidence that, indeed, there is a range of thermodynamic conditions where micelles form at the surface but not in the bulk. Subsequently, we study the properties of the surface micelles. The paper concludes with the compilation of the simulation results in a phase diagram.

II. Model and Simulation Technique

We perform Monte Carlo simulations in the framework of a coarse-grained lattice model of a dense polymer melt. In the bond fluctuation model (BFM),[23,24] linear, flexible macromolecules are represented by a string of N segments. Each segment occupies 8 lattice sites that constitute the vertices of a unit cube. Two consecutive segments are connected by fluctuating bonds, b, that can adopt the lengths 2, $\sqrt{5}$, $\sqrt{6}$, 3, and $\sqrt{10}$. With this choice, there are 108 possible bond vectors yielding a good approximation of continuum space. We study mixtures of asymmetric AB-diblock copolymers with homopolymers of the same length. The fraction of A segments in an AB-diblock copolymer is $f = {}^1/_8$. Thus, if the copolymers aggregate they will form spherical micelles at all concentrations. The solvent is represented by B-homopolymers. The total number density of segments is $8\phi = 0.5$, representing a dense melt with low compressibility. Both types of molecules—AB-diblocks and homopolymers—are comprised of the same number of effective segments, $N = 64$. Segments interact via a square well potential which is extended over the nearest 54 lattice sites.[25] Segments of the same type attract each other while segments of different type repel each other. Thus, the depth of the potential is given by $\varepsilon_{AA} = \varepsilon_{BB} = -\varepsilon_{AB} = -\varepsilon$ in units of the thermal energy scale, k_BT. For the strongly asymmetric amphiphiles, micelles form at rather large incompatibility. Like in our previous study[26] of micelles in the bulk, we consider $\varepsilon N \approx 20$ corresponding to the strong segregation regime, $\chi N \approx 100$.

In the z-direction, the system is confined between two parallel surfaces which are a distance $D = 96$ apart. In the x and y directions, we choose the same extension of the simulation box, $L_x = L_y = 96$, and apply periodic boundary conditions. The surfaces are hard, impenetrable and do not possess any lateral structure. They interact with A- and B-monomers via a square well potential that extends over the nearest two lattice layers. The strength of the interaction (in units of k_BT) is given by $\varepsilon_{AW} = -\varepsilon_W$ and $\varepsilon_{BW} = \varepsilon_W$, respectively. For $\varepsilon_W > 0$, the walls attract the minority component, A.

In order to equilibrate the morphology of the binary mixture, we work in the semigrandcanonical ensemble[25–28] where the total number of chains in the system $n_{AB} + n_B = n$ and the temperature T are fixed, but the composition $\phi_{AB} = n_{AB}/n$ fluctuates and is controlled by the exchange chemical potential $\delta\mu$. To this end, two kinds of moves are employed: (i) Random, local monomer displacements and slithering snakelike moves relax the coordinates of the macromolecules but leave the average composition unaltered. (ii) Identity switches AB $\rightleftharpoons$ B, which mutate a B-homopolymer into an AB-diblock copolymer, do not affect the molecular conformations but change the total composition.

The choice of the semigrandcanonical ensemble is crucial for the success of our simulations. Due to the "unphysical" identity switches, we establish chemical equilibrium between bulk and surface and the local composition of the mixture relaxes significantly faster compared to simulations in the canonical ensemble, where composition fluctuations decay via the slow diffusion of the long macromolecules in the melt. Moreover, the simulation cell would have to be intractably large for the volume to act as a reservoir, i.e., due to the small critical micelle concentration, the formation of a micelle would significantly change the bulk composition. Furthermore, the use of an explicit homopolymer solvent prevents large density fluctuations, and thus, we avoid the formation of dense, glassy cores of the micelle which hamper the investigation of micelles in solvent-free models. The efficiency of semigrandcanonical moves is demonstrated in Figure 1 where we compare the time evolution of the cluster size in simulations without (upper panel) and with (lower panel) identity switches for $\delta\mu = 5.9 < \delta\mu_{cmc}$(bulk) and $\varepsilon_W = 0.005$. Since the solubility of copolymers in the homopolymer solvent is vanishingly small, in the first case, the size of a surface micelle is almost constant, $\langle n_{AB}\rangle \approx 30$, while in the semigrandcanonical simulation it fluctuates around its mean value $\langle n_{AB}\rangle \approx 22$.

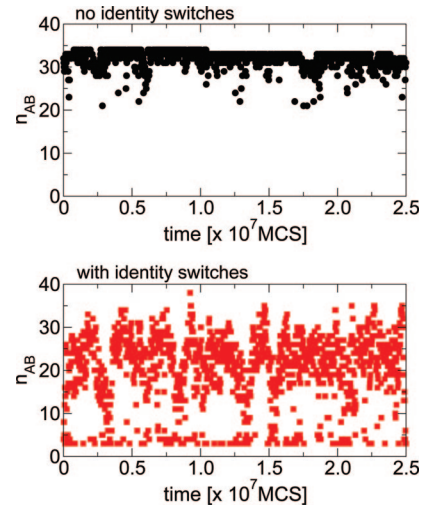

Figure 1. The upper panel shows the cluster size, n_{AB}, of a surface micelle in the simulation box as a function of time without identity switches for $\varepsilon_W = 0.005$ and $\delta\mu = 5.9$. The lower panel shows the simulation where identity switches are allowed for the same values of ε_W and $\delta\mu$.

III. Results

Adsorption Isotherms. In the semigrandcanonical ensemble the adsorption isotherm is directly accessible. In Figure 2 we vary the exchange chemical potential, $\delta\mu$, and observe the average concentration, ϕ_{AB}, of diblock copolymers in the film. At very small values of $\delta\mu$ the data follow a straight line on the semilogarithmic scale, $\ln \phi_{AB} \approx \delta\mu - \delta E$, which characterizes the solution of isolated diblock copolymers within mean-field theory for $\phi_{AB} \ll 1$. δE denotes the free energy associated with exchanging a B-homopolymer−solvent and an AB-diblock copolymer. Qualitatively, the adsorption behavior in a film parallels the isotherm in the bulk, which is also depicted in the figure. In the bulk, the free energy change is given by $\delta E = f\chi N$ as long as one has a dilute ideal solution of block copolymers. In the presence of a surface, this free energy change is significantly reduced. If the surface is hard and exhibits no preference, $\varepsilon_W = 0$, the A-segments adsorb to the surface because they have fewer B-segments in their surrounding ("missing neighbor" effect), i.e., the effective strength of attraction is not proportional to ε_W but also increases with the incompatibility, χN. If $\varepsilon_W < 0$ (results not shown in the figure), the adsorption is similar to the bulk and micelles at larger $\delta\mu$ form in the middle of the film. If $\varepsilon_W > 0$, A-segments additionally benefit from the attractive interaction with the surface, and they displace B-segments that are repelled.

The adsorption of the A-block at the surfaces results in a change of the block extensions parallel and perpendicular to the surface. In order to increase the favorable interactions the extension perpendicular to the surface decreases while the parallel chain extension increases. This behavior is shown in Figure 3, where we plot the ratio of parallel to perpendicular end-to-end-distance of the A-block. For the short A-block, there is some indication of an s-shaped variation in the vicinity of

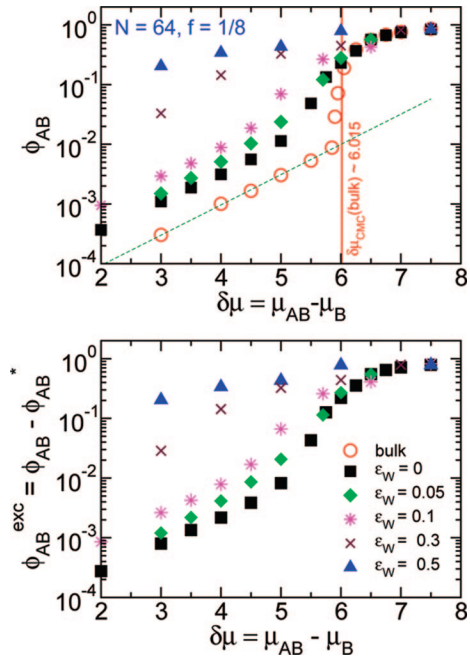

Figure 2. The upper panel shows the adsorption isotherms of copolymers in a confined system and the bulk for different strength of attraction ε_W between surface and minority component, A. ϕ_{AB} denotes the number of copolymers divided by the total number of chains in the system. The cmc in the bulk occurs at $\delta\mu_{cmc} \approx 6.015$ and it is marked by a full line. The dashed line given by $\phi^*_{AB} = 9.0631 \times 10^{-6}$ exp $(1.1671\delta\mu)$ is obtained by fitting the bulk data for small $\delta\mu$, in the isolated copolymers regime. In the lower panel we depict the excess concentrations of copolymers in the system, $\phi^{exc}_{AB} = \phi_{AB} - \phi^*_{AB}$.

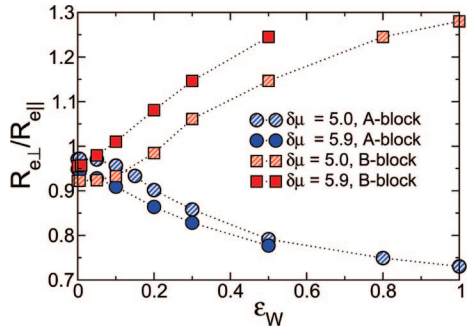

Figure 3. Plot showing the ratio between the parallel and the perpendicular end-to-end distance of the A- and B-blocks as a function of ε_W for $\delta\mu = 5.0$ and 5.9.

$\varepsilon_W \approx 0.15$. A transition can only emerge in the limit of large block length, and previous simulation studies[20,29] of adsorption from solution show that rather long chain lengths are required to observe the universal behavior. Nevertheless, it is interesting to note that the behavior resembles the one observed in polymer solutions adsorbing at a wall. The value of the ratio of parallel and perpendicular chain extensions is expected to be universal and the common intersection of ratios for different chain length might serve to locate the transition.

The adsorption of the AB-diblock copolymers at the surface, however, differs in two aspects from the adsorption transition of homopolymers from solution. First, the adsorbed A-block is covalently bound to a significantly longer B-block. As the A-blocks adsorb strongly, a brush of B-blocks is formed and the crowding of the chains limits the total amount of amphiphiles that can be adsorbed. For the short and very asymmetric amphiphiles considered in the present work, there is no extended regime where the A-block adsorbs but the B-block is unperturbed and not extended away from the surface. Second, since the solvent molecules and the AB-diblock copolymers are structurally symmetric in our model, they suffer a very similar loss of conformational entropy at the surface. At small adsorption, the conformation entropy loss of the polymers does not dictate the behavior because B-homopolymers are exchanged for AB-diblock copolymers.

Upon increasing the exchange chemical potential, the adsorption isotherm deviates from the ideal solution behavior exhibiting an s-shaped increase. At negative or very small values of ε_W, this behavior signals the rather abrupt formation of micelles in the bulk or the center of the film, respectively. The concentration of free amphiphiles (i.e., not belonging to an aggregate) in the bulk at $\delta\mu$ yields an estimate for the cmc. For chain length, $N = 64$, we obtain $\delta\mu_{cmc} \approx 6.015$. As we make the surface more attractive to A-blocks, the increase of concentration of amphiphiles becomes more gradual. In fact, for large values $\varepsilon_W \geq 0.3$, and the rather narrow film thickness considered in the simulation, the variation with the exchange chemical potential is rather smooth.

In the lower panel of Figure 2 we plot the excess concentration of copolymers, $\phi^{exc}_{AB} = \phi_{AB}(\delta\mu) - \phi^*_{AB}(\delta\mu)$ vs $\delta\mu$, where $\phi^*_{AB}(\delta\mu)$ is an estimate for the concentration of amphiphiles in the bulk solution not accounting for micelles. It is equal to the bulk concentration of amphiphiles below the cmc and is obtained by extrapolation for larger values of the exchange chemical potential, $\delta\mu$. This surface excess provides information about the adsorbed amount of amphiphiles and one observes a clear distinction between the behavior at small ε_W and larger values of the surface attraction.

Concentration Profiles. The adsorption isotherms indicate that the deviation from the ideal solution behavior is chiefly associated with the formation of an adsorption layer. The building up of an adsorbed layer is corroborated by the density profiles of the different species as a function of the distance from the surface. Figure 4 presents the data for different attraction strengths of the surface and two exchange chemical potentials. For a small exchange potential, $\delta\mu = 5.0$, there are hardly any copolymers in the center of the film. We observe a rather abrupt increase in the copolymer adsorption at the surface around $\varepsilon_W \approx 0.15$. This surface attraction marks the adsorption of A-blocks at the surface in agreement with the conclusion drawn from the extension of the A-blocks in Figure 3. Upon increasing ε_W further, the adsorbed amount of amphiphiles increases and a adsorbed brush is formed. The areal density of this adsorbed brush is dictated by a balance between the attraction between the A-heads and the surface and the loss of conformational entropy of the strongly stretched B-tails. For $\varepsilon_W \gg 0.15$, the B-tails of the amphiphiles form such a dense brush that the B-homopolymers are expelled from the surface and an interface between the B-brush and the B-homopolymer melt is generated. For an exchange potential that is only slightly below the cmc, $\delta\mu = 5.9 < \delta\mu_{cmc}$, the concentration of amphiphiles at the center of the film remains vanishingly small; the vast majority of amphiphiles is adsorbed on the surface. The adsorbed amount gradually increases with the attractive strength, ε_W, but already for the smallest value, $\varepsilon_W = 0.005$, there is a significant copolymer excess at the surface. For large values of ε_W, which correspond to an adsorbed brush, the behavior is rather insensitive to the exchange chemical potential. Note that a linear dimension $L = 96$ in the z-direction just suffices to avoid direct interaction between the brushes formed at the two opposing walls.

The formation of an adsorbed brush at small exchange potential also is clearly visible in the dependence of the surface excess of amphiphiles as a function of ε_W, which is presented in Figure 5. The graph depicts simulation results for different chemical potentials, $5 \leq \delta\mu \leq 6$, and two chain lengths, $N =$

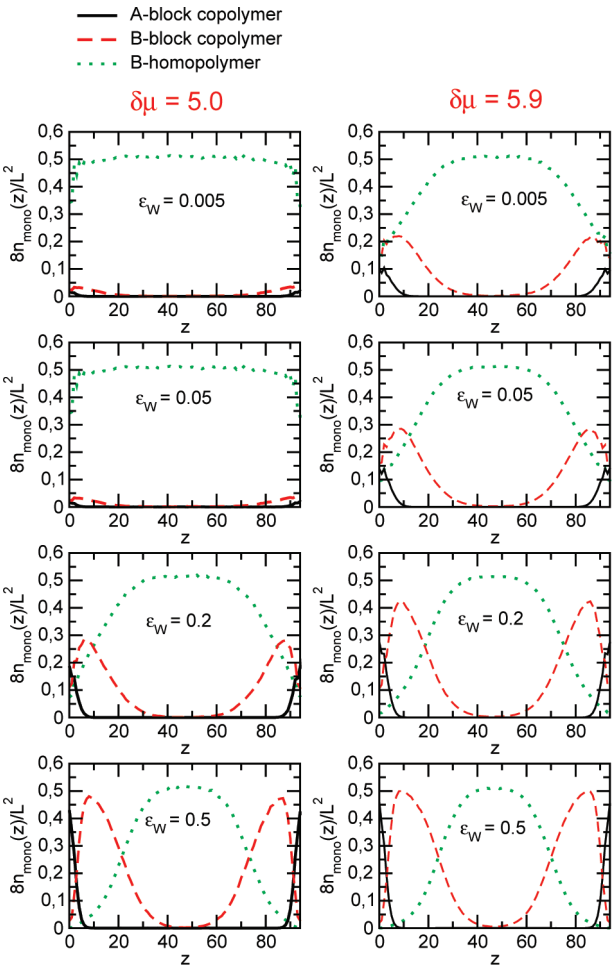

Figure 4. Density profiles of monomers as a function of the distance z from the walls at chemical potential $\delta\mu = 5.9$ and $5.0 < \delta\mu_{cmc}$ and different values of the wall interaction ε_W. The black (solid) lines denote A-segments, the red (dashed) ones depict B-blocks of the amphiphiles, while the green (dotted) curves describe the density profile of B-homopolymer chains.

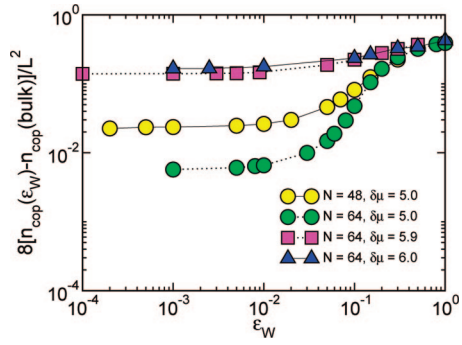

Figure 5. Plot showing the behavior of the surface excess monomer density as a function of the wall interaction on a logarithmic scale for different values of $\delta\mu$ and for $N = 48$ and 64.

64 and 48. The copolymer excess at the surface is presented on a logarithmic scale. The abrupt increase of surface excess around $\varepsilon_W \approx 0.15$ is the signature of the adsorption transition and it will sharpen further upon increasing the chain length. If the adsorbed layer is in chemical equilibrium with the bulk, adjusting the surface coverage to a specific value requires fine-tuning of the surface interactions. Closer to the bulk cmc, however, one observes a moderate surface coverage for an extended interval of surface interactions.

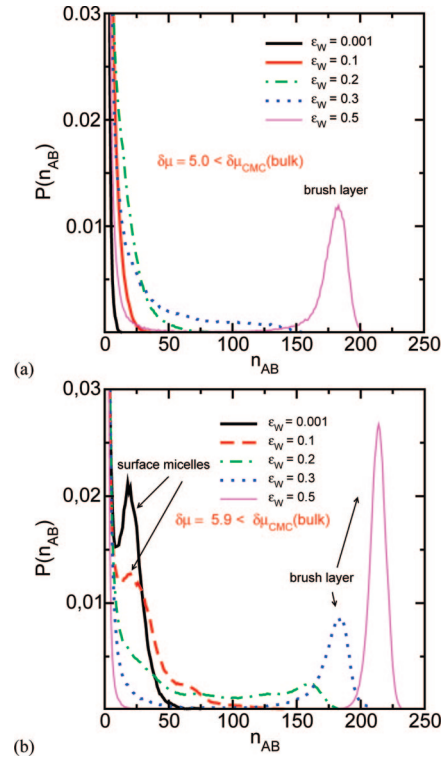

Figure 6. Cluster size distribution for (a) $\delta\mu = 5.0 \ll \delta\mu_{cmc}$ and (b) $\delta\mu = 5.9 \lesssim \delta\mu_{cmc}$. The peak centered at $n_{AB} = 1$, corresponds to isolated chains or very small and strongly fluctuating aggregates. Peaks around $n_{AB} \approx 25$ signal the presence of surface micelles with a well-defined size. The peak around $n_{AB} \geq 150$ marks the formation of a dense, adsorbed brush.

IV. Cluster Size

While the previous section studied the dependence of the surface excess on the bulk concentration and surface interaction, this section provides information about the structure of the adsorbed amphiphilic layer. At small surface excess, the adsorbed layer consists of isolated chains. At large surface excess, a dense brush is adsorbed. On the one hand, the cross-over between these two regimes could be completely gradual; i.e., the adsorbed chains aggregate into larger clusters, the size of the clusters gradually grows as one increases the attractive strength of the surface, they form a thin layer with strong local density fluctuations and, eventually, a dense adsorbed brush is built. This behavior parallels the adsorption of a homopolymer layer from solution. On the other hand, the amphiphilic nature of the molecules could give rise to surface micelles, i.e., aggregates with a well-defined size. Upon increasing the surface attraction, the number of surface micelles increases and their lateral interaction will give rise to lateral structure formation. Eventually, the areal density of surface micelles is so large that they will merge forming an adsorbed brush.

In Figure 6, we plot the distribution of cluster sizes as a function of the attraction of the surface far below the cmc (a) and close to it (b). In our definition, two amphiphiles belong to the same cluster if the distance of at least two A-monomers belonging to different chains is smaller or equal than the interaction range. In the first case, $\delta\mu = 5.0 \ll \delta\mu_{cmc}$, the cluster size distribution gradually extends to larger and larger sizes as we increase the strength of the attraction beyond $\varepsilon_W \approx 0.15$. However, no characteristic size that would correspond to a micelle can be identified. Configurational snapshots confirm that the aggregates do not possess the core-corona structure that is typical for micelles. For strong attractions, $\varepsilon_W > 0.3$, a peak

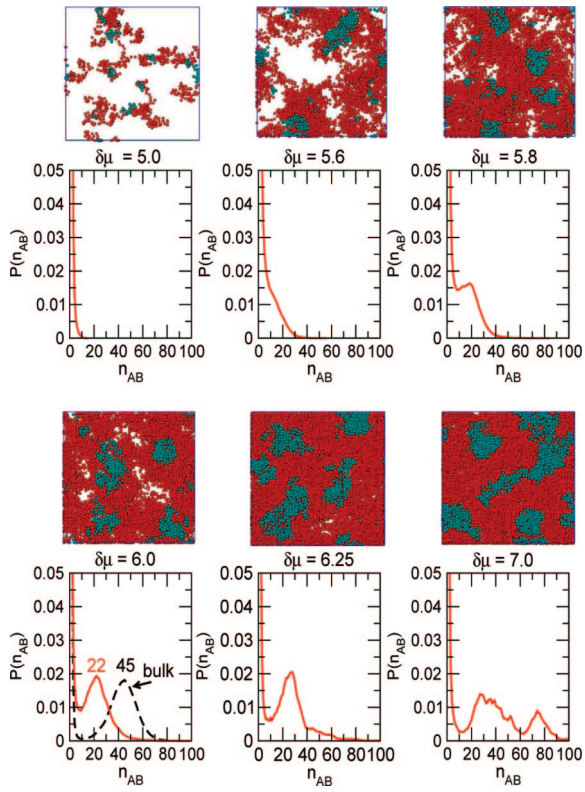

Figure 7. Cluster size distributions at $\varepsilon_w = 0.005$ and increasing values of $\delta\mu$ as indicated in the key. Above each plot are snapshots of the simulation box projected onto the $x-y$ plane. Here the dark (red) beads belong to B-blocks and the light (light blue) to A-blocks. B-homopolymers are not shown. For $\delta\mu = 5.9$, we compare the cluster size distribution of the confined system with the corresponding curve obtained in the bulk for $\delta\mu = 6.0$. This plot shows that, for a given $\delta\mu$ the mean size of bulk micelles is approximately double than the one of surface micelles.

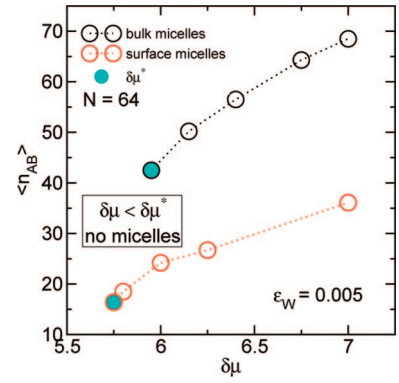

Figure 8. Average micelle size as a function of exchange potential.

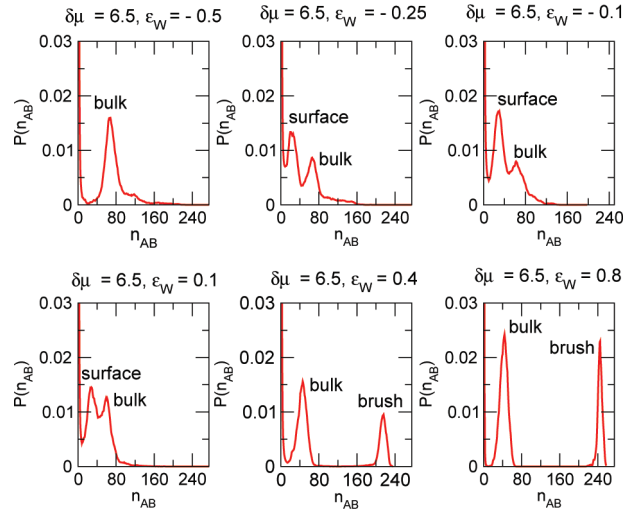

Figure 9. Cluster size distributions for $\delta\mu \approx 6.5$ and increasing values of ε_W as indicated in the key.

around $n_{AB} \approx 180$ is formed that corresponds to a dense, adsorbed brush.

The behavior is different close to the cmc. The simulation data in panel (b) correspond to $\delta\mu = 5.9 \lesssim \delta\mu_{cmc}$. At intermediate values of ε_W distinct peaks appear in the cluster size distribution, which indicate the formation of clusters of well-defined size. The configurational snapshots confirm that these clusters correspond to surface micelles where the A-block is adsorbed onto the surface and surrounded by a corona of B-tails. This structure prevents the gradual growth of the aggregates. At large surface attraction, a dense, adsorbed brush is formed.

In Figure 7, we plot the cluster size distribution for a small value of the surface attraction, $\varepsilon_W = 0.005$, as a function of the exchange chemical potential, $\delta\mu$. For $\delta\mu \ll \delta\mu_{cmc}$, one observes only isolated amphiphiles at the surface, while close to the cmc surface micelles form. The figure also contains data for $\delta\mu = 7 > \delta\mu_{cmc}$, where the cluster size distribution is comprised of two peaks, which are centered around $n_{AB} \approx 35$ and $n_{AB} \approx 75$. The former correspond to surface micelles while the latter peak characterizes the micelle size in the middle of the film.

Figure 8 shows how the size of the surface and bulk micelles depend on the exchange potential, $\delta\mu$. Surface micelles already form below the cmc, thus the data for the surface micelles start at lower values of $\delta\mu$. Upon increasing $\delta\mu$, we observe that both bulk and surface micelles increase in size, but their size ratio remains approximately constant.

The dependence of the micelle size beyond the cmc, $\delta\mu = 6.5 > \delta\mu_{cmc}$ is illustrated in Figure 9. In this case, micelles of size $n_{AB} \approx 60$ are present at the center of the film. If the surface strongly repels the core block A and attracts the corona block B, $\varepsilon_W \leq -0.5$, no surface micelles can be observed. For a small negative value, $-0.25 \leq \varepsilon_W \leq 0$, micelles form at the surface (due to the "missing neighbor effect"). Their size slightly increases with ε_W and their probability increases. For strong surface attraction, a dense adsorbed brush is formed as indicated by the peak around $n_{AB} \approx 220$. Upon increasing the surface attraction further, the brush becomes thicker. For the film thickness used in the simulations, the size of the bulk micelles slightly decreases as we increase the surface interaction. This effect stems from the finite film thickness; as both film surfaces are covered with surface micelles or an adsorbed brush, the micelles in the middle of the film—the "bulk"—becomes slightly squeezed.

V. Surface Micelles Properties

In this section, we will focus on the conformational properties of surface micelles for a given chemical potential $\delta\mu$ and increasing strength of the attraction between A-monomers and the surfaces. As shown in Figure 6, for $\delta\mu = 5.9$ and increasing ε_W, below the adsorption transition, i.e. for $\varepsilon_W < 0.15$, the average size of surface micelles is nearly constant, $\langle n_{AB} \rangle \approx 20$, nevertheless, quantities like the parallel and perpendicular components of radius of gyration of the micelle with respect to the walls, the shape or the contact angle of the core with the surface will be affected by increasing the strength of the attraction between the core and the walls. All quantities shown in this section are obtained selecting the size window, $n_{AB} = \langle n_{AB} \rangle \pm 5$.

As first step, we measure the parallel and perpendicular components, $R_{g\parallel} \equiv (R_{gx} + R_{gy})/2$ and $R_{g\perp} \equiv R_{gz}$, respectively, of the radius of gyration of core and corona as a function of ε_W

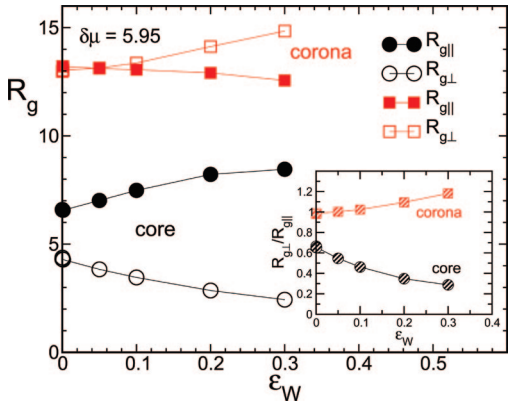

Figure 10. Parallel and perpendicular components of the radius of gyration, $R_{g\|}$ and $R_{g\perp}$ of core and the corona of a surface micelle as a function of the wall interaction ε_W for a given chemical potential $\delta\mu = 5.95$. The inset shows that ratio $R_{g\perp}/R_{g\|}$ vs ε_W.

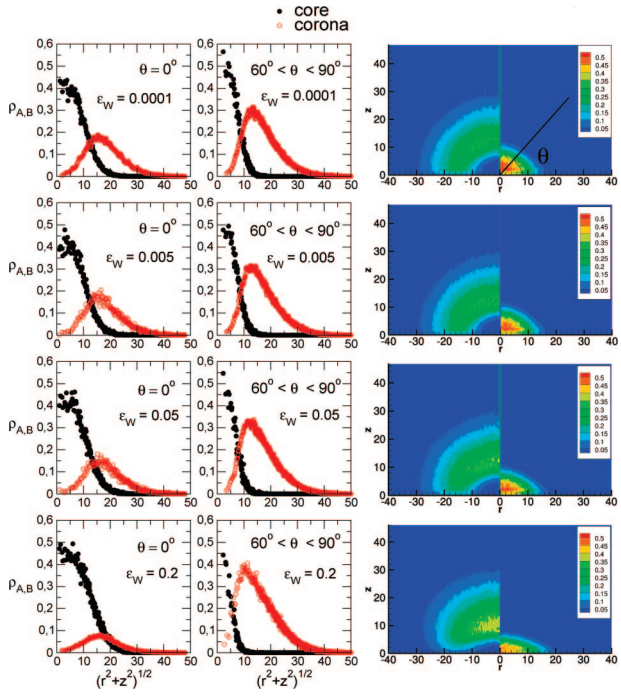

Figure 11. Cylindrically averaged density profiles of core, ρ_A, and corona, ρ_B for $0.0001 \le \varepsilon_W \le 0.2$ and fixed chemical potential, $\delta\mu = 5.9$. The left column presents density profiles parallel to the surface on the plane $z = 0$. The right column shows the results as a function of the distance from the micelle center averaged over angles θ towards the r-axis in the interval $30^o < \theta < 90^o$. In the third column, we show the corresponding two-dimensional contour plots. The angle θ is illustrated in the right upper panel.

for $\delta\mu = 5.95$. The results are plotted in Figure 10. For weak interaction with the surface, $\varepsilon_W < 0.1$, the parallel and perpendicular components of R_g are unperturbed by the surface. Upon increasing the strength of the attractive potential for the A-monomers forming the core, we observe that the component of the radius of gyration parallel to the walls increases and, due to the incompressibility of the core, the perpendicular component decreases. When $\varepsilon_W > 0.1$, the component perpendicular to the walls, increases approximately by 6%. This is a direct consequence of the stretching of the B-block due to brush formation as can be seen in Figure 3. The inset shows that ratio between parallel and perpendicular components of R_g vs ε_W.

The behavior of the micelle extension parallel and perpendicular to the surface as a function of ε_W for $\delta\mu = 5.9$ is visualized in Figure 11, where we plot the density profiles of

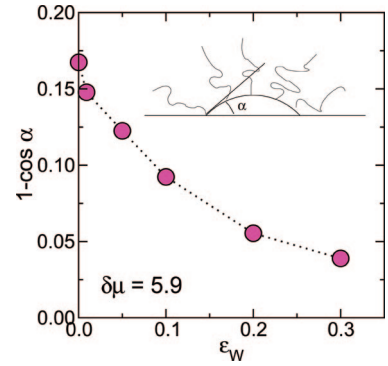

Figure 12. $1 - \cos\alpha$, where α is the contact angle of the core with the wall (see sketch), is plotted as a function of ε_W. The chemical potential is $\delta\mu = 5.9$.

core and corona in the r–z plane, where $r = (x^2 + y^2)^{1/2}$ and z denotes the distance from the surface. The profiles have been averaged cylindrically around the z-axis. This is a simplification, and its validity will be assessed in the last part of this section. Only the density of core and corona segments are shown, the data for the homopolymer–solvent are not depicted. In the first column, we plot the radial profile of core, ρ_A, and corona, ρ_B, along the horizontal r-axis in the plane $z = 0$, the middle column depicts profiles along an axis that makes the angle θ with the horizontal r-axis. The data are averaged over a cone with $60^o < \theta < 90^o$. The third column shows the corresponding contour plots in two dimensions. The profiles reveal that only for $0.05 < \varepsilon_W < 0.2$ the shape of the surface micelle significantly changes; above $\varepsilon_W = 0.05$ the core starts to flatten and, at the same time, monomers belonging to B-blocks are expelled from the surface. The largest value, $\varepsilon_W = 0.2$, is very close to the cross-over from isolated surface micelles to a dense, adsorbed brush.

This crossover occurs close to the value of the surface interaction where the A-monomers wet the surface. In Figure 12, we plot $1 - \cos\alpha$, α being the contact angle defined as the angle between the tangent to the core and the r-axis (see sketch). The wetting transition in a symmetric binary blend would occur at $\varepsilon_W^* \approx (\chi b^2/96)^{1/2} = 0.39$ in the strong segregation limit.[30] For the accessible range of surface interactions the contact angle of the micellar core is always less than that of a large droplet according to Young's equation. This observation is in qualitative agreement with the theoretical model of Ligoure.[11] Note that we cannot measure the contact angle for $\varepsilon_W > 0.2$ because, above this value, a dense, adsorbed layer is gradually formed. Therefore, there exists a minimum accessible contact angle which for our model is $\theta_{min} \approx 16^o$.

By the same token, if one considers a state with $\delta\mu > \delta\mu_{cmc}$, and $\varepsilon_W \le 0.1$ (i.e., below the adsorption transition), where surface micelles are present at the walls together with a layer of bulk micelles in the center of the film, one will observe a detachment of the micelles from the surface upon decreasing ε_W. This effect corresponds to dewetting.

In the following, we will focus on the shape of the surface micelles projected on the x–y plane. In order to study the anisotropy of the cluster we evaluated the eigenvalues, $g_\|^{min}$ and $g_\|^{max}$ ($g_\|^{min} < g_\|^{max}$), of the gyration tensor, $g_\|$, in the direction parallel to the wall. The components of the gyration tensor in the x–y plane are defined as $g_{\|,\alpha\beta} = (1/2N^2)\sum_{ij}[r_{i,\alpha} - r_{j,\alpha}][r_{i,\beta} - r_{j,\beta}]$ where $r_{i,\alpha}$ is the α-component of the position of the ith monomer in a given chain ($i = 1,\ldots, N$; $\alpha = x, y$). Note that $R_{gx}^2 + R_{gy}^2 = g^{min} + g^{max}$. A measure of the projected shape of the cluster is given by the asphericity, A, defined as follows: $A = (g^{max} - g^{min})^2/(g^{max} + g^{min})^2$. A assumes values from 0 to 1. If $A = 0$, the projected micelle will exhibit a spherical symmetry.

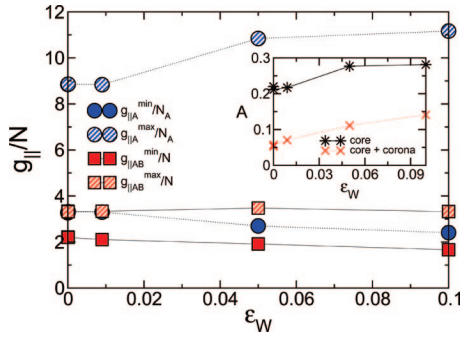

Figure 13. Eigenvalues of the gyration tensor parallel to the walls and the corresponding values of the asphericity (inset) as a function of ε_W for $\delta\mu = 5.9$. $g_{A||}$ refers to the core of the surface micelle ($N_A = 8$ is the A-block length) and $g_{AB||}$ to the whole micelle ($N = 64$ is the total chain length).

For $A = 1$, the cluster will be strongly elongated, i.e., a rod or a cylinder.

In Figure 13, we plot the two eigenvalues divided by the chain length vs ε_W. We show the result for monomers belonging to the core (labeled A) and for monomers belonging to the whole micelle (labeled AB). In the first case, we divide the eigenvalues by the A-block length, $N_A = 8$, in the second one normalizes by the total chain length $N = 64$. For the core, we see that there is a large discrepancy between the 2 eigenvalues, this is a clear sign of the fact that the projected shape is not isotropic. The difference augments with increasing attraction between A-monomers and the walls. The asphericity of the core also increases with ε_W and the absolute values, $0.2 < A < 0.3$, are characteristic of rather anisotropic objects. This behavior is also born out by the asphericity that is depicted in the inset. For the whole micelle, this effect is less evident and the asphericity is approximately a factor of 2 smaller than for the core.

This observation is quite surprising because in the bulk we observe micelles with asphericity $A \approx 10^{-3}$. For large ε_W, the shape of the core is certainly affected by the interaction with neighboring micelles and the largest values of the asphericity in the interval $0.1 < \varepsilon_W < 0.2$ signal the gradual crossover between surface micelles and a dense, adsorbed brush.

VI. Concluding Remarks

Using Monte Carlo simulations of a coarse-grained lattice model, we have studied micellization in thin films. The use of the semigrandcanonical ensemble enabled us to equilibrate micelles of long, asymmetric amphiphiles and to study the adsorption of the amphiphiles at the surface in equilibrium with a bulk solution. Our qualitative findings are summarized in the diagram of states presented in Figure 14 as a function of the exchange chemical potential $\delta\mu$ and the wall interaction ε_W. As alternative, on the opposite axis, we have introduced an alternative couple of variables, which is more meaningful for comparisons with experiments: the equivalent bulk copolymer concentration, ϕ_{AB}(bulk), and the dimensionless spreading parameter, S, defined as $b^2(\Delta\gamma - \gamma_{AB})/k_BT = \rho b^3(2d_w b^{-1}\varepsilon_W - [\chi/6]^{1/2})$, where $\Delta\gamma = 2d_w\rho\varepsilon_W$ is the difference of surface tension of pure A and B components ($d_w = 2$ is the range of the surface interaction) and $\gamma_{AB} = \rho b[\chi/6]^{1/2}$, the surface tension in the strong segregation limit, which is appropriate for the present simulations. The diagram shows that far below the cmc, amphiphiles adsorb in an unstructured way which is similar to the adsorption transition of A-homopolymers at the surface. No surface micelles are observed. Close but below the cmc, adsorbed amphiphiles form surface micelles, and the cross-over from a few isolated chains to surface micelles occurs at the lower surface attraction the larger the bulk concentration of amphiphiles. Above the cmc, both, surface micelles and bulk micelles, are observed. If the attraction of the surface for the minority component is very large, unstructured aggregates at the surface or surface micelles merge to form a dense, adsorbed brush. Upon increasing the attraction further, the adsorbed brush becomes denser and the amphiphiles stretch away from the surface due to their steric interactions.

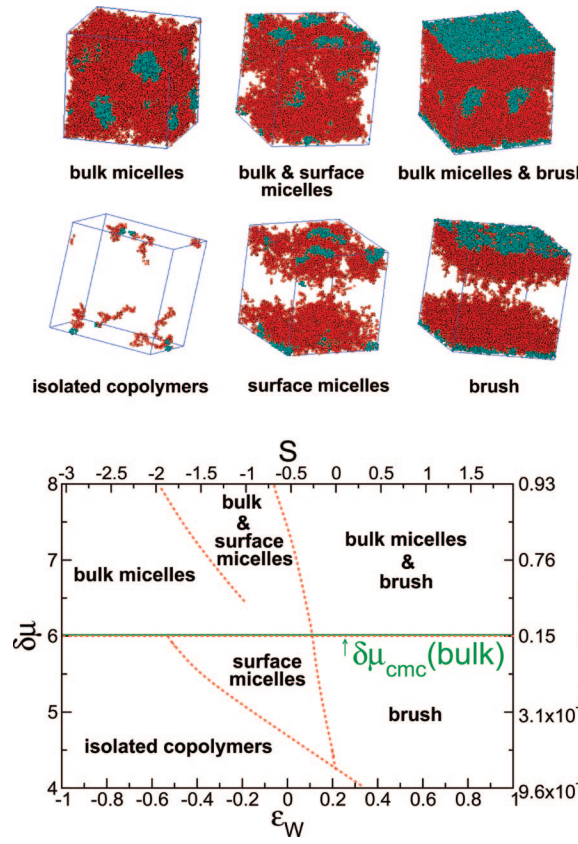

Figure 14. Diagram of states as a function of the control variables, exchange chemical potential $\delta\mu$ and wall interaction ε_W. On the opposite sides, we indicate the alternative variables, $S = \rho b^3(2d_w\varepsilon_W b^{-1} - [\chi/6]^{1/2})$, the dimensionless spreading parameter, and ϕ_{AB}(bulk), the equivalent bulk concentration.

Acknowledgment. We thank C. Pastorino, J. P. Wittmer, A. Johner, and J. Baschnagel for stimulating and helpful discussions. Financial support was provided by MPI-P Mainz and ESF project STIPOMAT. The simulations were performed at the JCS Jülich, the ZDV Mainz, and the GWDG Göttingen.

References and Notes

(1) Leibler, L. *Macromolecules* **1982**, *15*, 1283–1290.
(2) Leibler, L. *Makromol. Chem.—Macromol. Symp.* **1988**, *16*, 1–17.
(3) Shull, K. R.; Kramer, E. J. *Macromolecules* **1990**, *23*, 4769–4779.
(4) Matsen, M. W. *J. Chem. Phys.* **1999**, *110*, 4658–4667.
(5) Müller, M.; Gompper, G. *Phys. Rev. E* **2002**, *66*, 041805.
(6) Shull, K. R.; Winey, K. I.; Thomas, E. L.; Kramer, E. J. *Macromolecules* **1991**, *24*, 2748–2751.
(7) Zhan, Y. J.; Mattice, W. L. *Macromolecules* **1994**, *27*, 683–688.
(8) Connell, S. D.; Collins, S.; Fundin, J.; Yang, Z.; Hamley, I. W. *Langmuir* **2003**, *19*, 10449–10453.
(9) Hamley, I. W.; Connell, S. D.; Collins, S. *Macromolecules* **2004**, *37*, 5337–5351.

(10) Toomey, R.; Mays, J.; Yang, J. C.; Tirrell, M. *Macromolecules* **2006**, *39*, 2262–2267.
(11) Ligoure, C. *Macromolecules* **1991**, *24*, 2968–2972.
(12) Singh, C.; Zhulina, E. B.; Gersappe, D.; Pickett, G. T.; Balazs, A. C. *Macromolecules* **1996**, *29*, 7637–7640.
(13) Potemkin, I. I.; Kramarenko, E. Y.; Khokhlov, A. R.; Winkler, R. G.; Reineker, P.; Eibeck, P.; Spatz, J. P.; Möller, M. *Langmuir* **1999**, *15*, 7290–7298.
(14) Milchev, A.; Binder, K. *Langmuir* **1999**, *15*, 3232–3241.
(15) Spatz, J. P.; Mössmer, S.; Hartmann, C.; Möller, M.; Herzog, T.; Krieger, M.; Boyen, H. G.; Ziemann, P.; Kabius, B. *Langmuir* **2000**, *16*, 407–415.
(16) Spatz, J. P.; Mössmer, S.; Möller, M.; Kramarenko, E. Y.; Khalatur, P.; Potemkin, I. I.; Khokhlov, A. R.; Winkler, R. G.; Reineker, P. *Macromolecules* **2000**, *33*, 150–157.
(17) Albrecht, K.; Mourran, A.; Möller, M. *Adv. Polym. Sci.* **2006**, *200*, 57–70.
(18) Dewhurst, P. F.; Lovell, M. R.; Jones, J. L.; Richards, R. W.; Webster, J. R. P. *Macromolecules* **1998**, *31*, 7851–7864.
(19) Maaloum, M.; Muller, P.; Krafft, M. P. *Angew. Chem., Int. Ed.* **2002**, *41*, 4331–4334.
(20) Eisenriegler, E.; Kremer, K.; Binder, K. *J. Chem. Phys.* **1982**, *77*, 6296–6320.
(21) Leibler, L.; Orland, H.; Wheeler, J. C. *J. Chem. Phys.* **1983**, *79*, 3550−3557.
(22) Noolandi, J.; Hong, K. M. *Macromolecules* **1983**, *16*, 1443–1448.
(23) Carmesin, I.; Kremer, K. *Macromolecules* **1988**, *21*, 819–2823.
(24) Müller, M. *Macromol. Theory Simul.* **1999**, *8*, 343–374.
(25) Müller, M.; Binder, K. *Macromolecules* **1995**, *28*, 1825–1834.
(26) Cavallo, A.; Müller, M.; Binder, K. *Macromolecules* **2006**, *39*, 9539–9550.
(27) Sariban, A.; Binder, K. *J. Chem. Phys.* **1987**, *86*, 5859–5873.
(28) Müller, M.; Schick, M. *J. Chem. Phys.* **1996**, *105*, 8885–8901.
(29) Metzger, S.; Müller, M.; Binder, K.; Baschnagel, J. *Macromol. Theory Simul.* **2002**, *11*, 985–995.
(30) Müller, M.; Binder, K. *Macromolecules* **1998**, *31*, 8323–8346.

MA800262F